Heliyon 9 (2023) e22276

Contents lists available at ScienceDirect

Heliyon

journal homepage: www.cell.com/heliyon

A dual-channel fluorescence probe for simultaneously visualizing cysteine and viscosity during drug-induced hepatotoxicity

Ya-Long Zheng *, Ruixue Yu, Mengbo Li, Cailian Fan, Li Liu, Huijie Zhang, Wenqian Kang, Run Shi, Changzhi Li, Yarui Li, Jiaqi Wang, Xinhua Zheng **

Medicine College of Pingdingshan University, Pingdingshan, Henan 467000, China

ARTICLE INFO

Keywords:
Fluorescence probe
Dual-channel
Cysteine
Viscosity
Hepatotoxicity

ABSTRACT

Cysteine (Cys), one of the important participants in protecting cells from oxidative stress, is closely associated with the occurrence and development of various diseases. Moreover, cell viscosity as a pivotal microenvironmental parameter has recently attracted increasing attention due to its dominant role in governing intracellular signal transduction and diffusion of reactive metabolites. Thus, simultaneous detection of Cys and viscosity is imperative for investigating their pathophysiological functions and cross-link. Herein we present a mitochondria-targetable dual-channel fluorescence probe **ABDSP** by grafting the acrylate modified pyridinium unit to dimethylaminobenzene. Whilst the probe is a seemingly simple, it could simultaneously discriminate Cys and viscosity in a fashion of distinguishable signals. Furthermore, the probe was successfully employed for visualizing mitochondrial Cys and viscosity, and probe into their cross-link during acetaminophen-induced hepatotoxicity.

1. Introduction

Biothiols, mainly including cysteine (Cys), homocysteine (Hcy) and glutathione (GSH), stand out as the second messengers of oxidative stress, and function as important players in redox homeostasis, signal transduction and metabolic regulation in biological system [1–3]. They harbor similar chemical properties owing to their similar chemical structures, but play different roles in some physiological events. Apart from being the biosynthesis precursors of GSH and sulfur-containing proteins [4], Cys also participates in maintaining the biological conformation of protein, and mediates the body's intestinal function, lipid metabolism and other processes [5–7]. It is worth noting that Cys is tightly related to the occurrence and development of various diseases. Excessive Cys could induce Alzheimer's disease, Rheumatoid arthritis and Parkinson's disease, while deficient Cys will result in retarded growth, liver damage, edema and skin damage [8–10].

On one hand, the growth, proliferation and normal physiological function of cells are inseparable from the balance of redox homeostasis [11,12]; on the other hand, the multiple biological activities of cells are closely related to the microenvironments [13–15]. Cellular microenvironmental factors mainly include polarity, viscosity and pH, where viscosity acts as a key biomarker to engage in signal transduction, electron transport and biomolecule interaction [15–19]. The abnormal variation of cell viscosity may lead to the occurrence of multitudinous diseases including malignant tumor, diabetes, Alzheimer's disease and atherosclerosis [15,20–22].

* Corresponding author.
** Corresponding author.
E-mail addresses: m17337531022@163.com (Y.-L. Zheng), xinhuazheng@pdsu.edu.cn (X. Zheng).

https://doi.org/10.1016/j.heliyon.2023.e22276
Received 16 August 2023; Received in revised form 6 November 2023; Accepted 8 November 2023
Available online 11 November 2023

Additionally, there is a close correlation between intracellular viscosity and redox homeostasis, such as an increase viscosity induced by oxidative stress. Thus, considering the vital cross-link between redox signaling molecules and cellular microenvironment parameters in biological system, it is of great significance to develop a powerful tool for simultaneously detecting them.

Nowadays, fluorescence imaging has attracted a great deal of attention owing to the superior performance of simple operation, nondestructive detection, high temporal-spatial resolution and excellent sensitivity [23–28]. However, only a few fluorescence probes were employed for simultaneously monitoring Cys and viscosity [29–32], and it is still imperative to develop a single probe to differentiate them simultaneously by the distinguishable signals. Accordingly, we constructed a dual-channel fluorescence probe **ABDSP** to simultaneously detect Cys and viscosity, and visualize their interconnectedness in the pathological process. The probe features the 4-*p*-dimethylaminostyrylpyridinium and acrylate, which serve as viscosity response unit and Cys recognition site, respectively (Scheme 1A). We reasoned that probe **ABDSP** could exhibit green fluorescence with Cys owing to the DPA generation through the addition-cyclization reaction of the probe and Cys [33], and red fluorescence with viscosity by the suppression of the twisted intramolecular charge transfer (TICT) process [34,35]. Indeed, the sulfhydryl group of Cys can attack the probe **ABDSP** to form a thioether, and then amino group undergo intramolecular cyclization to generate the cyclized thiolactam product, which is accompanied by a subsequent 1,6-elimination reaction of the *p*-hydroxybenzyl moiety to release the free fluorophore DPA (Scheme 1B). Meanwhile, viscosity could induce a turn-on fluorescence enhancement of the probe **ABDSP** at 613 nm due to the suppression of the single-bond rotation between dimethylaminobenzene and vinylpyridinium.

2. Materials and methods

2.1. Synthesis of *ABDSP*

The probe **ABDSP** was easily prepared by 4-step reactions following the synthetic routes shown in Scheme S1, and its synthesis details and characterization were included in the Supporting Information.

2.2. Optical studies

The probe **ABDSP** was dissolved in DMSO for preparing the stock solution (10 mM), and then diluted to 10 μM in optical response experiments. Biothiols and anions were dissolved in deionized water to prepare the stock solution with a concentration of 100 mM, and metal ions were dissolved in deionized water for preparing the stock solution (50 mM). Subsequently, the analytes were diluted to the

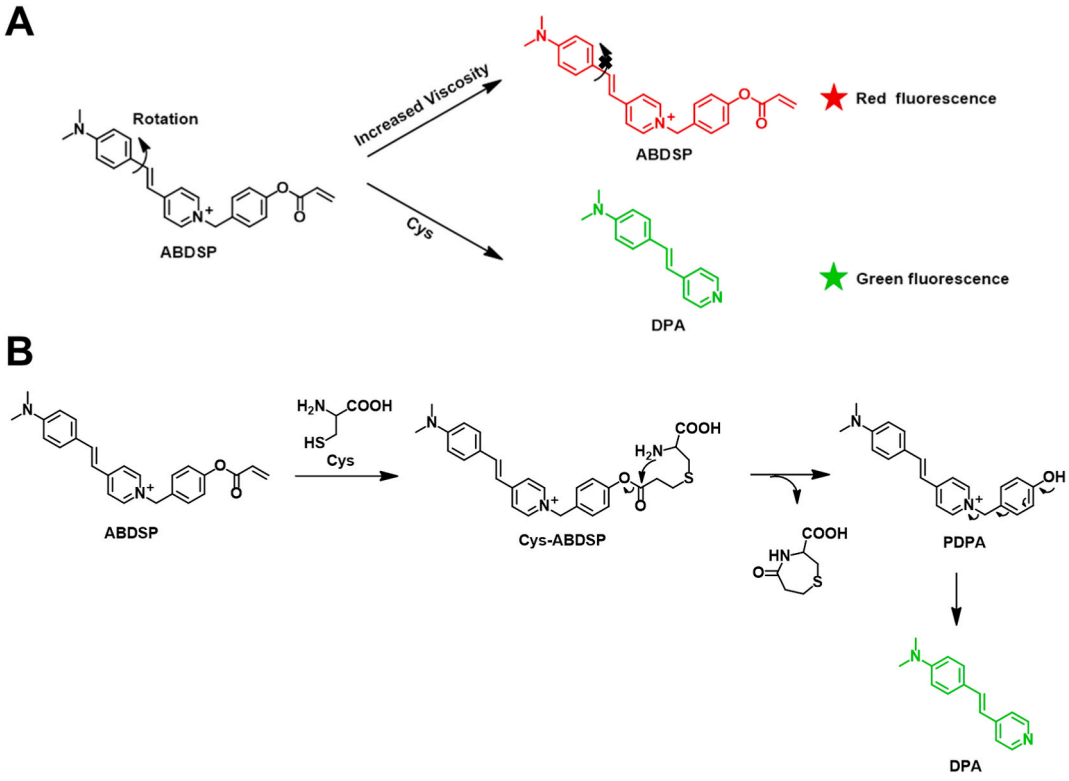

Scheme 1. Rational design of a dual-channel fluorescence probe **ABDSP**. (A) Molecular structure of **ABDSP** and its mechanism for simultaneously detecting Cys and viscosity. (B) The detailed mechanisms of probe **ABDSP** response to Cys.

desired concentration with PBS for the optical response experiments. Moreover, the viscosity response experiments were carried out in the mixed solvent of PBS and glycerol. The UV/vis absorption and fluorescence response spectra were recorded using the TU-1901 and F-7000 FL spectrophotometer, respectively. The excitation and emission slit width were set at 10 nm and 20 nm, respectively.

2.3. Cytotoxicity of probe *ABDSP*

The cytotoxicity of probe **ABDSP** was evaluated by the standard 3-(4,5-dimethylthiazol-2-yl)-2,5-diphenyltetrazolium bromide (MTT) assay. HepG2 cells purchased from the Shanghai Institute of Biochemistry and Cell Biology (Shanghai, China), were cultured in RPMI 1640 medium including 10 % fetal bovine serum (FBS), 100 U/mL penicillin, and 100 U/mL streptomycin, and grown at 37 °C in a humidified 5 % CO_2 incubator. Subsequently, the cells (5×10^3 cells/well) harvested from culture flasks were seeded into 96-well plates and adhered for overnight, followed by treatment with different concentrations of probe **ABDSP** for 24 h. Removing the culture medium, the cells were incubated with RPMI 1640 medium containing 0.5 mg/mL MTT for another 4 h. The OD values were acquired by Tecan Infinite M200 microplate reader.

2.4. Cell imaging

HepG2 cells were seeded into 6-well culture plates at a density of 2×10^5 cells/well and allowed to resume exponential growth for overnight. For imaging of Cys, the cells were treated with different concentrations of Cys for 30 min, and further incubated with the probe **ABDSP** for 30 min. To image viscosity, HepG2 cells were sequentially treated with nystatin (30 min) and probe **ABDSP** (30 min). To image the acetaminophen (APAP)-induced hepatotoxicity, HepG2 cells were treated with APAP for 12 h, followed by incubation with probe **ABDSP** for 30 min, and NAC pretreatment for 1 h if necessary. After treatment in various ways, the cells were washed with PBS and imaged by fluorescence microscope (Leica DMI 4000B, Germany).

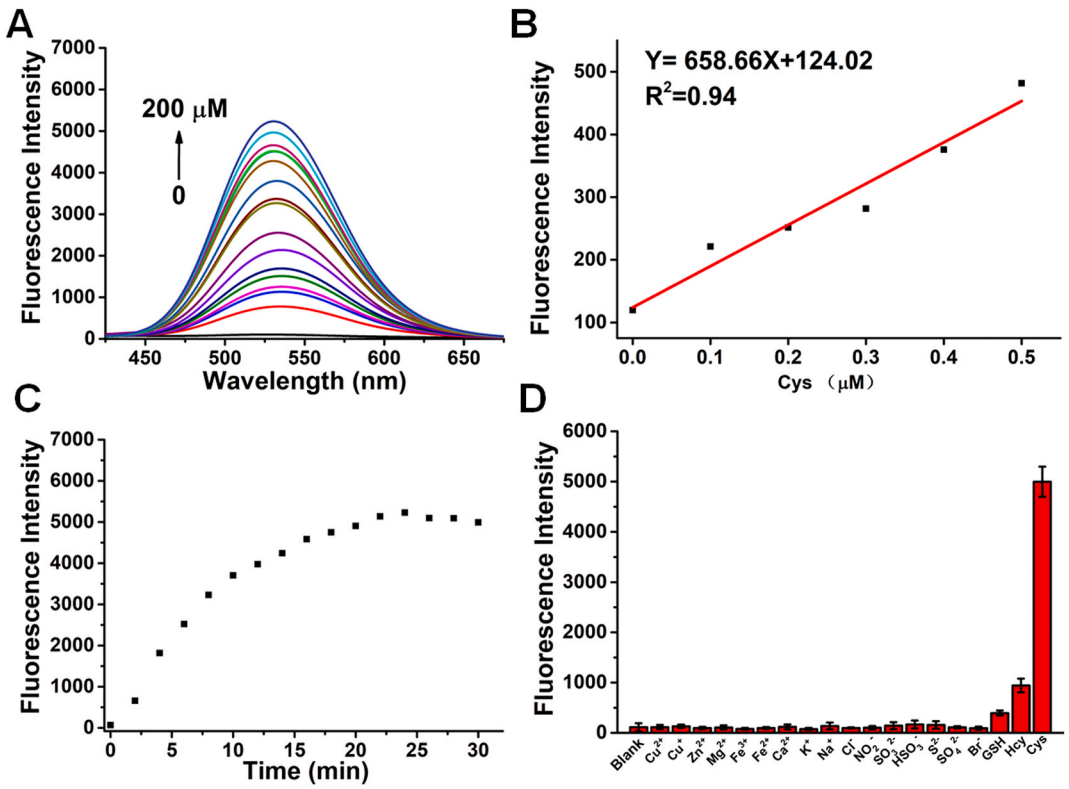

Fig. 1. Optical response of **ABDSP** toward Cys. (A) Fluorescence emission spectra of **ABDSP** (10 μM) upon addition of Cys (0–200 μM) in PBS/DMSO buffer (1/1, v/v). (B) Linear relationship between the intensity at 530 nm and Cys concentrations. (C) Changes in fluorescence intensity of probe **ABDSP** (10 μM) at 530 nm over time in the presence of Cys (200 μM). (D) Fluorescence response of **ABDSP** (10 μM) at 530 nm toward GSH (1 mM), Cys (200 μM) and other analytes (100 μM) in PBS/DMSO buffer (1/1, v/v). λ_{ex} = 380 nm, slit (nm): 10/20.

3. Results and discussion

3.1. Optical response to Cys

With **ABDSP** in hand, we initially evaluated the responsive ability of probe toward Cys using a UV/vis absorption spectrometer. As shown in Fig. S1, the probe displayed an obvious absorption peak at 488 nm. Upon addition of Cys, the original UV/Vis absorption peak decreased significantly as well as the emergence of a new absorption peak at about 380 nm. Meanwhile, the probe alone showed a negligible fluorescence emission upon excitation at 380 nm but manifested a fluorescence enhancement at 530 nm in the presence of Cys with a large Stokes shift (150 nm) (Fig. 1A). These changes of the probe in absorption and fluorescence spectra were assigned to the release of the corresponding fluorophore DPA *via* Cys-mediated addition-cyclization reaction. Subsequently, a good linear relationship between probe fluorescence intensity at 530 nm and Cys concentration was revealed, and the detection limit was calculated to be 8.8 nM based on 3σ/k method, highlighting the superior sensitivity of probe **ABDSP** to Cys (Fig. 1B). The reaction-time experiment was also carried out, and the fluorescence signals gradually increased and reached the steady state within 25 min after adding 200 μM Cys (Fig. 1C). To investigate the effect of pH value on the probe, we conducted the pH titration experiments. As shown in Fig. S2, the probe itself was stable in a pH range of 4.0–10.0, but exhibited a strong fluorescence response to Cys under physiological conditions, supporting the biological application of probe **ABDSP**. Additionally, we further evaluated the selectivity of probe **ABDSP** toward Cys in the presence of various relevant interfering substances including biothiols, metal ions and anions. As shown in Fig. 1D, Cys caused a remarkable enhancement of fluorescence intensity at 530 nm in comparison with other test species, stressing the excellent specificity of the probe to Cys.

Next, the reaction mechanism was further explored using absorption spectrum, fluorescence spectrum and mass spectroscopy. As shown in Fig. S3, the mixture of probe **ABDSP** response to Cys exhibited the strong absorption at 380 nm and fluorescence emission at 530 nm, which was consistent with the characteristic absorption and fluorescence emission of the fluorophore DPA (Figs. S3A and B). Moreover, the reaction products of probe **ABDSP** with Cys were also analyzed by mass spectrometry, and the main molecular ion peak (m/z = 225.1979, $[M + H]^+$) corresponding to the fluorophore DPA was observed (Fig. S3C). Meanwhile, we also detected the mass peak of the intermediate product, such as m/z = 506.3046 and 331.2535 assigned to the Cys-adduct (Cys-ABDSP) and phenol intermediate (PDPA), respectively. According to these data, we could reason that the probe first undergoes an addition reaction with Cys to produce the adduct (Cys-ABDSP), followed by the cyclization reaction to release the phenol intermediate (PDPA) and the elimination reaction to obtain the fluorophore DPA. These results are in line with the proposed mechanism shown in Scheme 1.

3.2. Optical response to viscosity

Firstly, the UV/Vis absorption changes of the probe in viscous and non-viscous medium were investigated. It can be seen from Fig. S4 that the absorption peak of probe **ABDSP** displayed a slight red shift from 488 to 498 nm in viscous glycerol system compared to PBS/DMSO buffer, which was attributed to the restriction of molecular rotation. Secondly, the fluorescence property of the probe was measured in different viscosity. As shown in Fig. 2A, the probe exhibited the faint background fluorescence in PBS, while the fluorescence signal of probe **ABDSP** gradually enhanced as the rising glycerol ratio and reached its maximum value in pure glycerol. Notably, the fluorescence emission of the probe at 613 nm enhanced 136-fold. Finally, probe **ABDSP** exhibited negligible fluorescence response in non-viscous environment (Fig. 2B). The above data demonstrate that probe **ABDSP** could serve as a potential tool for monitoring viscosity.

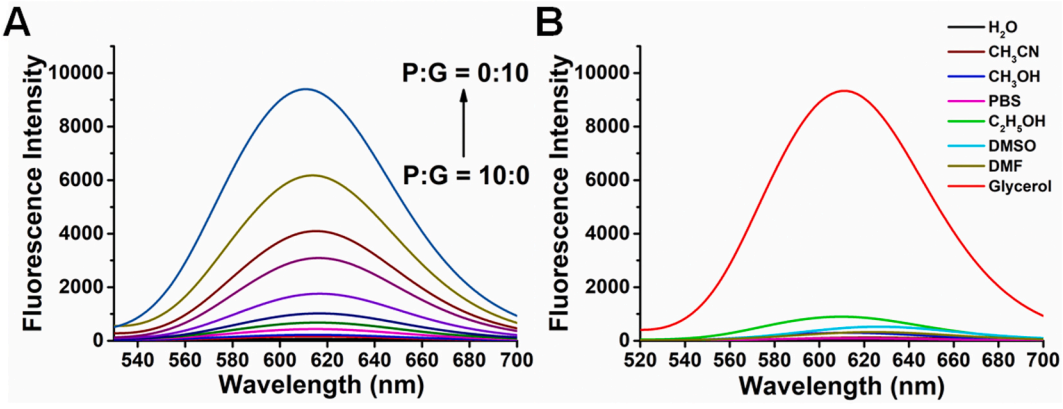

Fig. 2. (A) Fluorescence spectra of **ABDSP** (10 μM) in different ratios of PBS (P) and glycerol (G) mixtures. (B) Fluorescence spectra of **ABDSP** (10 μM) in different solvents. λ_{ex} = 498 nm, slit (nm): 10/20.

3.3. Cytotoxicity and colocalization experiment

Prior to colocalization experiment, the cytotoxicity of probe **ABDSP** against HepG2 cells was tested through the standard MTT assay, and the results showed that the probe possessed low cytotoxicity at the concentration up to 20 μM (Fig. S5). Accordingly, we selected the probe with a concentration of 5 μM for subsequent colocalization experiment and cell imaging. As shown in Fig. 3, the fluorescence of Mito-Tracker Green (a commercialized mitochondrial dye) in green channel overlapped well with that of probe **ABDSP** in red channel (Fig. 3A–C), and Pearson's colocalization coefficient was determined as 0.87 (Fig. 3D), hinting the excellent mitochondria-targeting capacity of the probe.

3.4. Cell imaging

With the aid of probe **ABDSP**, the fluorescence experiments for imaging intracellular Cys were then conducted. As shown in Fig. 4A, cells only treated with probe **ABDSP** presented the weak green fluorescence, indicating that the probe is capable of tracking mitochondrial basal Cys. Upon addition of Cys, cells exhibited the significantly enhanced fluorescence signals in the green channel along with a dose-dependent fashion, implying that the probe can monitor the fluctuation of mitochondrial Cys levels. In addition, nystatin could disrupt the ionic balance of cells, cause mitochondrial dysfunction, and increase viscosity [36,37]. As shown in Fig. 4B, compared to the cells directly incubated with the probe, that pretreated with nystatin and then stained **ABDSP** displayed a strong red fluorescence, and the fluorescence intensity increased with the increasing dosages of nystatin. When the cells were treated with nystatin at the same concentration for different time, the gradually enhanced red fluorescence signal was observed over time (Fig. S6), demonstrating a time-dependent relationship between fluorescence intensity of probe **ABDSP** and nystatin. Furthermore, the photostability of probe **ABDSP** in living cells has also been evaluated by treating cells with Cys and nystatin, respectively. Fig. S7 showed that the green and red fluorescence intensity remain unchanged within 10 min, highlighting that probe **ABDSP** has a good photostability. Collectively, the above results support that probe **ABDSP** can simultaneously detect Cys and viscosity in a well-separated dual-channel mode.

3.5. Drug-induced hepatotoxicity

APAP is a commonly used pain killer and antipyretic drug [38,39], and can induce hepatotoxicity by an extensive oxidative stress, leading to the increase of viscosity and the irreversible depletion of Cys [39,40]. To visualize the changes of viscosity and Cys in the process of hepatotoxicity, we used APAP as an inducer for the following fluorescence imaging experiments. As shown in Fig. 5, there was a bright green fluorescence and weak red fluorescence in the cells exclusively incubated with probe **ABDSP** (Fig. 5a1-a3). After treating with APAP and then staining with probe **ABDSP**, the cells showed the obvious decrease of green fluorescence signal and remarkable enhancement of red fluorescence signal (Fig. 5b1-b3), whereas the pretreatment with NAC (a classic antioxidant) reversed clearly the fluorescence changes induced by APAP (Fig. 5c1-c3). These data visualized the internal relationship between Cys and viscosity during APAP-induced hepatotoxicity, that is, oxidative stress led to the decrease of Cys level and increase of viscosity, illustrating that probe **ABDSP** can be beneficial for imaging the toxicity mechanism of APAP.

4. Conclusions

In summary, we designed and synthesized a dual-functional fluorescence probe **ABDSP** for simultaneously detecting Cys and viscosity by virtue of the distinct signals: green for Cys and red for viscosity. Probe **ABDSP**, with superior sensitivity (detection limit = 8.8 nM), a large Stokes shift (150 nm) and excellent selectivity toward Cys, and 136-fold red fluorescence enhancement toward viscosity, was successfully employed to visualize mitochondrial Cys and viscosity in living cells. More importantly, the probe was first applied to probe into the mutual relevance between Cys and viscosity during APAP-induced hepatotoxicity. We expect that the probe would be a promising tool for further understanding the roles of Cys and viscosity under different pathophysiological conditions.

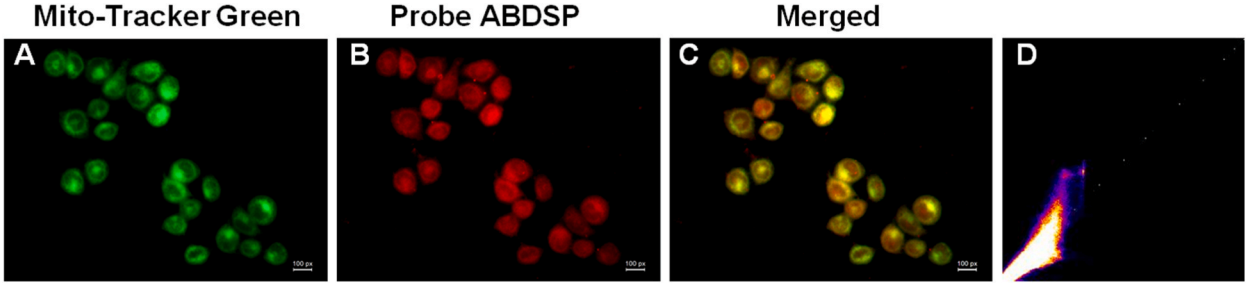

Fig. 3. Intracellular localization of **ABDSP**. (A–C) Fluorescence images of HepG2 cells treated with **ABDSP** (5 μM, 30 min) and subsequently stained with Mito-Tracker Green (50 nM, 30 min). Green channel: λ_{ex} = 460–500 nm, λ_{em} = 512–542 nm. Red channel: λ_{ex} = 515–560 nm, λ_{em} = 590–630 nm. (D) Scatter plot: the correlation plots of green and red channels.

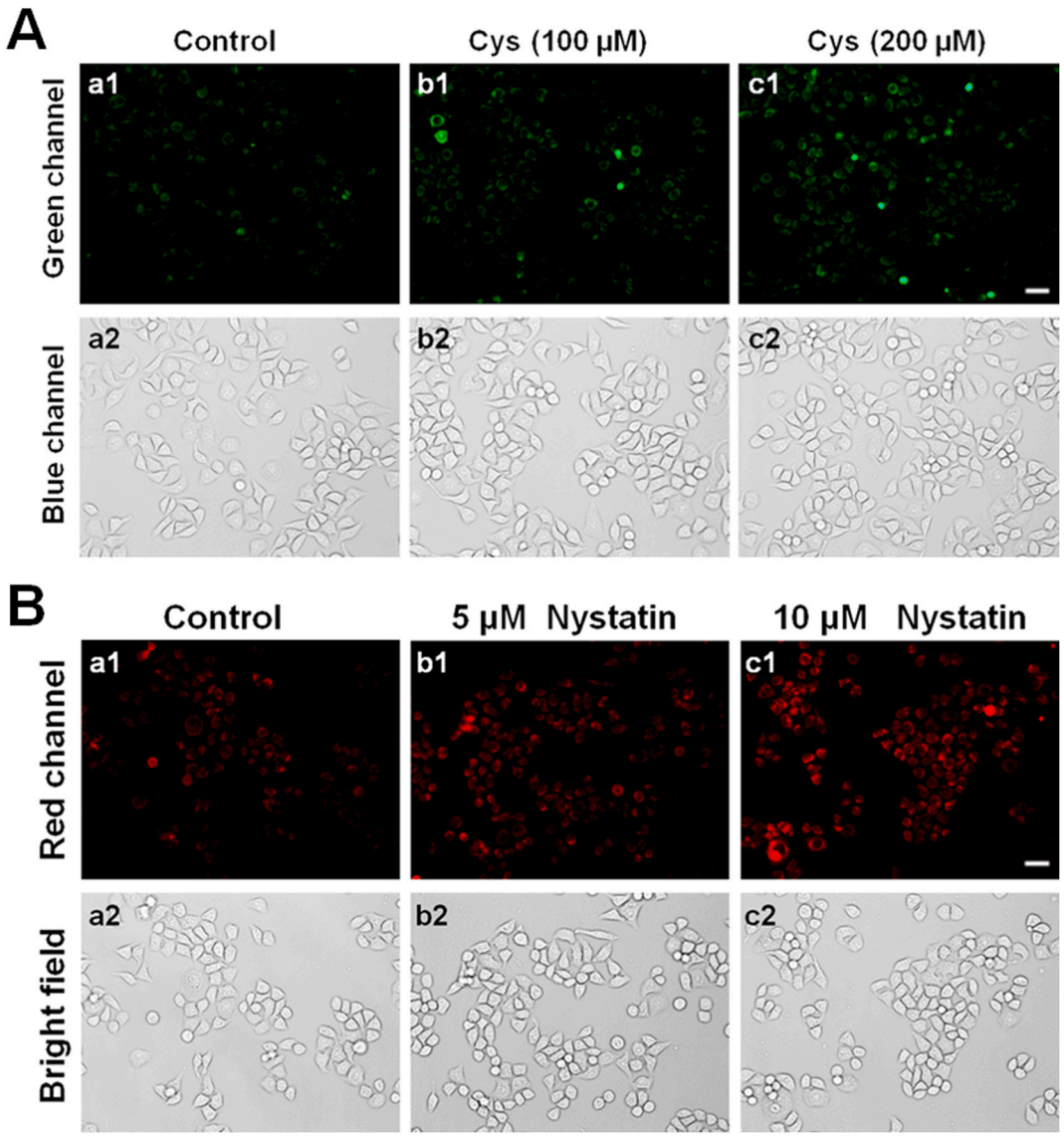

Fig. 4. Cellular imaging of Cys and viscosity. (A) (a1, a2) HepG2 cells were treated only with **ABDSP** (5 μM) for 30 min (b1, b2, c1 and c2) HepG2 cells were treated with Cys (100 or 200 μM) for 30 min and then incubated with **ABDSP** (5 μM) for another 30 min. Scale bar: 25 μm. λ_{ex} = 460–500 nm, λ_{em} = 512–542 nm. (B) (a1, a2) HepG2 cells were only incubated with **ABDSP** (5 μM) for 30 min (b1, b2, c1 and c2) HepG2 cells were treated with nystatin (5 or 10 μM) for 30 min and then incubated with **ABDSP** (5 μM) for another 30 min. Scale bar: 25 μm. λ_{ex} = 515–560 nm, λ_{em} = 590–630 nm.

Data availability statement

Data will be made available on request.

CRediT authorship contribution statement

Ya-Long Zheng: Writing – review & editing, Writing – original draft, Visualization, Validation, Supervision, Project administration, Investigation, Data curation, Conceptualization. **Ruixue Yu:** Visualization, Project administration, Investigation, Data curation. **Mengbo Li:** Project administration, Investigation, Data curation. **Cailian Fan:** Validation, Supervision, Investigation, Data curation. **Li Liu:** Validation, Supervision, Investigation. **Huijie Zhang:** Investigation, Formal analysis, Data curation. **Wenqian Kang:** Supervision, Investigation, Formal analysis, Data curation. **Run Shi:** Formal analysis, Data curation. **Changzhi Li:** Investigation, Data curation. **Yarui Li:** Validation, Data curation. **Jiaqi Wang:** Validation, Data curation. **Xinhua Zheng:** Writing – original draft, Visualization, Supervision, Project administration, Data curation, Conceptualization.

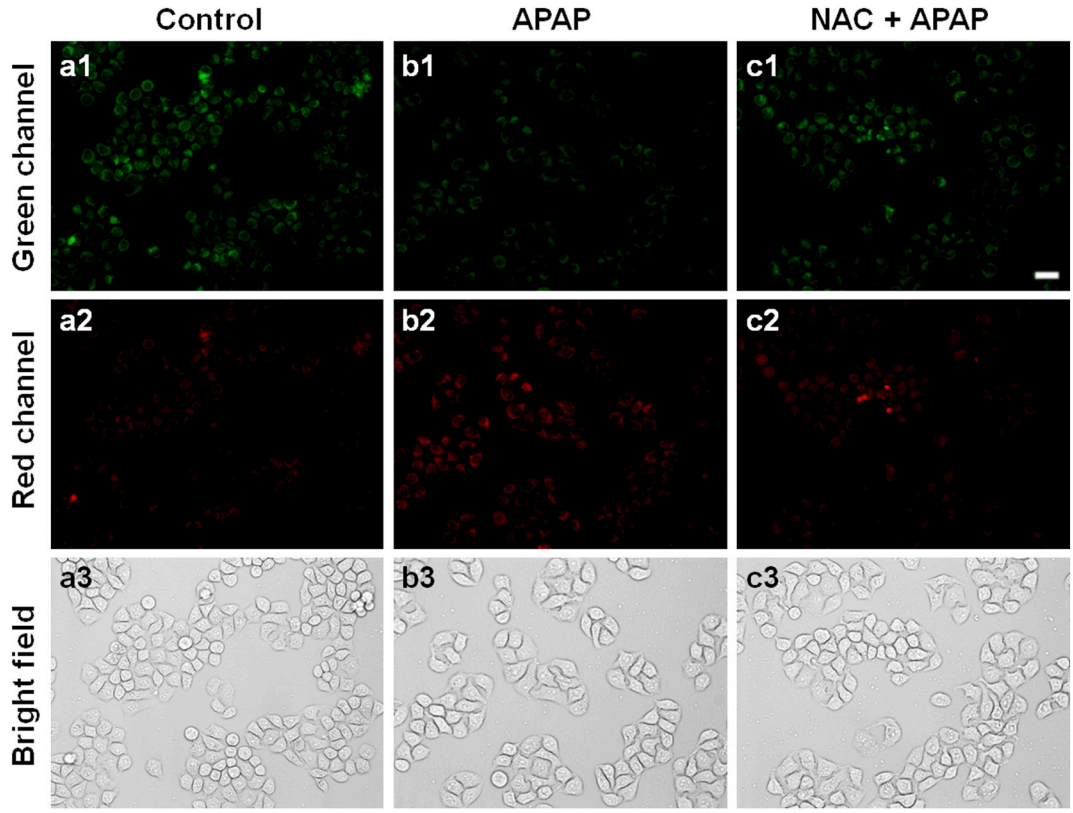

Fig. 5. Fluorescence images of APAP-induced hepatotoxicity. (a1-a3) HepG2 cells were directly incubated with **ABDSP** (5 μM, 30 min) as control. (b1-b3) HepG2 cells were stimulated with APAP (500 μM, 12 h) and incubated with **ABDSP** (5 μM, 30 min). (c1-c3) HepG2 cells were successively incubated with NAC (1 mM, 1 h), APAP (500 μM, 12 h) and **ABDSP** (5 μM, 30 min). Scale bar: 25 μm. Green channel: λ_{ex} = 460–500 nm, λ_{em} = 512–542 nm. Red channel: λ_{ex} = 515–560 nm, λ_{em} = 590–630 nm.

Declaration of competing interest

The authors declare that they have no known competing financial interests or personal relationships that could have appeared to influence the work reported in this paper.

Acknowledgements

This work was supported by Henan Engineering Technology Research Center of Funiu Mountain Medicinal Resource Utilization and Molecular Medicine, Key Scientific Research Projects of Higher Education Institutions in Henan Province (No. 22B310009), Key Science and Technology Research Projects in Henan Provincial (No. 232102310460) and Pingdingshan College PhD Startup Fund under Grant (Nos. PXY-BSQD-2023020, PXY-BSQD-2022040, PXY-BSQD-2022037 and PXY-BSQD-2023021).

Appendix A. Supplementary data

Supplementary data to this article can be found online at https://doi.org/10.1016/j.heliyon.2023.e22276.

References

[1] G.I. Giles, K.M. Tasker, C. Jacob, Hypothesis: the role of reactive sulfur species in oxidative stress, Free Radical Biol. Med. 31 (2001) 1279–1283.
[2] T.V. Mishanina, M. Libiad, R. Banerjee, Biogenesis of reactive sulfur species for signaling by hydrogen sulfide oxidation pathways, Nat. Chem. Biol. 11 (2015) 457–464.
[3] V.S. Lin, W. Chen, M. Xian, C.J. Chang, Chemical probes for molecular imaging and detection of hydrogen sulfide and reactive sulfur species in biological systems, Chem. Soc. Rev. 44 (2015) 4596–4618.
[4] L. He, X. Yang, K. Xu, X. Kong, W. Lin, A multi-signal fluorescent probe for simultaneously distinguishing and sequentially sensing cysteine/homocysteine, glutathione, and hydrogen sulfide in living cells, Chem. Sci. 8 (2017) 6257–6265.
[5] C.E. Paulsen, K.S. Carroll, Cysteine-mediated redox signaling: chemistry, biology, and tools for discovery, Chem. Rev. 113 (2013) 4633–4679.

[6] R. Zhang, J. Yong, J. Yuan, Z.P. Xu, Recent advances in the development of responsive probes for selective detection of cysteine, Coord. Chem. Rev. 408 (2020), 213182.
[7] S.P. Baba, A. Bhatnagar, Role of thiols in oxidative stress, Curr. Opin. Toxicol. 7 (2018) 133–139.
[8] Y. Yue, F. Huo, P. Ning, Y. Zhang, J. Chao, X. Meng, C. Yin, Dual-site fluorescent probe for visualizing the metabolism of Cys in living cells, J. Am. Chem. Soc. 139 (2017) 3181–3185.
[9] Y.-M. Go, D.P. Jones, Cysteine/cystine redox signaling in cardiovascular disease, Free Radic. Biol. Med. 50 (2011) 495–509.
[10] R. Janaky, V. Varga, A. Hermann, P. Saransaari, S.S. Oja, Mechanisms of L-cysteine neurotoxicity, Neurochem. Res. 25 (2000) 1397–1405.
[11] L. Wu, A.C. Sedgwick, X. Sun, S.D. Bull, X.-P. He, T.D. James, Reaction-based fluorescent probes for the detection and imaging of reactive oxygen, nitrogen, and sulfur species, Acc. Chem. Res. 52 (2019) 2582–2597.
[12] Y. Long, J. Liu, D. Tian, F. Dai, S. Zhang, B. Zhou, Cooperation of ESIPT and ICT processes in the designed 2-(2′-hydroxyphenyl)benzothiazole derivative: a near-infrared two-photon fluorescent probe with a large Stokes shift for the detection of cysteine and its application in biological environments, Anal. Chem. 92 (2020) 14236–14243.
[13] J. Park, B. Lim, N.K. Lee, J.H. Lee, K. Jang, S.W. Kang, S. Kim, I. Kim, H. Hwang, J. Lee, Dual-functioning IQ-LVs as lysosomal viscosity probes with red-shifted emission and inhibitors of autophagic flux, Sens. Actuators B Chem. 309 (2020), 127764.
[14] C. Ma, W. Sun, L. Xu, Y. Qian, J. Dai, G. Zhong, Y. Hou, J. Liu, B. Shen, A minireview of viscosity-sensitive fluorescent probes: design and biological applications, J. Mater. Chem. B 8 (2020) 9642–9651.
[15] Z. Yang, J. Cao, Y. He, J.H. Yang, T. Kim, X. Peng, J.S. Kim, Macro-/micro-environment-sensitive chemosensing and biological imaging, Chem. Soc. Rev. 43 (2014) 4563–4601.
[16] J. Guo, B. Fang, H. Bai, L. Wang, B. Peng, X.-J. Qin, L. Fu, C. Yao, L. Li, W. Huang, Dual/Multi-responsive fluorogenic probes for multiple analytes in mitochondria: from design to applications, Trends Anal. Chem. 155 (2022), 116697.
[17] J. Yin, L. Huang, L. Wu, J. Li, T.D. James, W. Lin, Small molecule based fluorescent chemosensors for imaging the microenvironment within specific cellular regions, Chem. Soc. Rev. 50 (2021) 12098–12150.
[18] X. Yang, D. Zhang, Y. Ye, Y. Zhao, Recent advances in multifunctional fluorescent probes for viscosity and analytes, Coord. Chem. Rev. 453 (2022), 214336.
[19] H. Wang, Y. Sun, X. Lin, W. Feng, Z. Li, M. Yu, Multi-organelle-targeting pH-dependent NIR fluorescent probe for lysosomal viscosity, Chin. Chem. Lett. 34 (2023), 107626.
[20] A. Zheng, H. Liu, X. Gao, K. Xu, B. Tang, A mitochondrial-targeting near-infrared fluorescent probe for revealing the effects of hydrogen peroxide and heavy metal ions on viscosity, Anal. Chem. 93 (2021) 9244–9249.
[21] X. Zhang, Q. Sun, Z. Huang, L. Huang, Y. Xiao, Immobilizable fluorescent probes for monitoring the mitochondria microenvironment: a next step from the classic, J. Mater. Chem. B 7 (2019) 2749–2758.
[22] S. Wang, W.X. Ren, J.-T. Hou, M. Won, J. An, X. Chen, J. Shu, J.S. Kim, Fluorescence imaging of pathophysiological microenvironments, Chem. Soc. Rev. 50 (2021) 8887–8902.
[23] D. Cheng, Y. Pan, L. Wang, Z. Zeng, L. Yuan, X. Zhang, Y.-T. Chang, Selective visualization of the endogenous peroxynitrite in an inflamed mouse model by a mitochondria-targetable two-photon ratiometric fluorescent probe, J. Am. Chem. Soc. 139 (2017) 285–292.
[24] S. Singha, Y.W. Jun, S. Sarkar, K.H. Ahn, An endeavor in the reaction-based approach to fluorescent probes for biorelevant analytes: challenges and achievements, Acc. Chem. Res. 52 (2019) 2571–2581.
[25] P. Gao, W. Pan, N. Li, B. Tang, Fluorescent probes for organelle-targeted bioactive species imaging, Chem. Sci. 10 (2019) 6035–6071.
[26] S. Li, F. Huo, C. Yin, NIR fluorescent probe for dual-response viscosity and hydrogen sulfide and its application in Parkinson's disease model, Dyes Pigments 197 (2022), 109825.
[27] H. Song, W. Zhang, Y. Zhang, C. Yin, F. Huo, Viscosity activated NIR fluorescent probe for visualizing mitochondrial viscosity dynamic and fatty liver mice, Chem. Eng. J. 445 (2022), 136448.
[28] W. Zhang, Y. Lv, F. Huo, Y. Zhang, C. Yin, Viscosity-sensitive NIR probe for in vivo imaging of early-stage hepatic fibrosis, J. Mater. Chem. B 10 (2022) 8852–8855.
[29] M. Fu, K. Wang, Q. Ma, J. Zhu, M. Bian, Q. Zhu, A novel dual-functional fluorescent probe for imaging viscosity and cysteine in living system, Org. Biomol. Chem. 20 (2022) 672–677.
[30] S.K. Samanta, K. Maiti, S. Halder, U.N. Guria, D. Mandal, K. Jana, A.K. Mahapatra, A 'double locked' ratiometric fluorescent probe for detection of cysteine in a viscous system and its application in cancer cells, Org, Biomol. Chem. 21 (2023) 575–584.
[31] L. Niu, T. Zhang, H. Zhao, H. Dong, Y. Zhang, T. Liang, J. Wang, Simultaneous imaging of Cysteine and viscosity in living cells with sharp contrast fluorescence between red and green by a dual-responsive fluorescence probe, Dyes Pigments 206 (2022), 110610.
[32] S. Li, F. Huo, Y. Wen, C. Yin, A dual-response NIR probe reveals positive correlation between biothiols and viscosity under cellular stress change, Chem. Commun. 58 (2022) 4881–4884.
[33] S. Li, D. Song, W. Huang, Z. Li, Z. Liu, In situ imaging of cysteine in the brains of mice with epilepsy by a near-infrared emissive fluorescent probe, Anal. Chem. 92 (2020) 2802–2808.
[34] S.-J. Li, Y.-F. Li, H.-W. Liu, D.-Y. Zhou, W.-L. Jiang, J. Ou-Yang, C.-Y. Li, A dual-response fluorescent probe for the detection of viscosity and H_2S and its application in studying their cross-talk influence in mitochondria, Anal. Chem. 90 (2018) 9418–9425.
[35] C. Wang, W. Chi, Q. Qiao, D. Tan, Z. Xu, X. Liu, Twisted intramolecular charge transfer (TICT) and twists beyond TICT: from mechanisms to rational designs of bright and sensitive fluorophores, Chem. Soc. Rev. 50 (2021) 12656–12678.
[36] M. Ren, B. Deng, K. Zhou, X. Kong, J.-Y. Wang, W. Lin, Single fluorescent probe for dual-imaging viscosity and H_2O_2 in mitochondria with different fluorescence signals in living cells, Anal. Chem. 89 (2017) 552–555.
[37] Y.-L. Zheng, X.-C. Li, W. Tang, L. Xie, F. Dai, B. Zhou, A coumarin-based fluorescent probe: small but multi-signal, Sens. Actuators B Chem. 368 (2022), 132169.
[38] K. Du, A. Ramachandran, H. Jaeschke, Oxidative stress during acetaminophen hepatotoxicity: sources, pathophysiological role and therapeutic potential, Redox Biol. 10 (2016) 148–156.
[39] P. Zhou, M. She, P. Liu, S. Zhang, J. Li, Measuring the distribution and concentration of cysteine by fluorescent sensor for the visual study of paracetamol-induced pro-sarcopenic effect, Sens. Actuators B Chem. 318 (2020), 128258.
[40] Y. Deng, G. Feng, Visualization of $ONOO^-$ and viscosity in drug-induced hepatotoxicity with different fluorescence signals by a sensitive fluorescent probe, Anal. Chem. 92 (2020) 14667–14675.